

DİoT: A Self-learning System for Detecting Compromised IoT Devices

Thien Duc Nguyen
TU Darmstadt,
Germany
ducthien.nguyen@trust.tu-
darmstadt.de

Samuel Marchal
Aalto University,
Finland
samuel.marchal@aalto.fi

Markus Miettinen
TU Darmstadt,
Germany
markus.miettinen@trust.tu-
darmstadt.de

N. Asokan
Aalto University
Finland
asokan@acm.org

Ahmad-Reza Sadeghi
TU Darmstadt,
Germany
ahmad.sadeghi@trust.tu-
darmstadt.de

ABSTRACT

IoT devices are being widely deployed. Many of them are vulnerable due to insecure implementations and configuration. As a result, many networks *already* have vulnerable devices that are easy to compromise. This has led to a new category of malware specifically targeting IoT devices. Existing intrusion detection techniques are not effective in detecting compromised IoT devices given the massive scale of the problem in terms of the number of different types of devices and manufacturers involved.

In this paper, we present DİoT, a system for detecting compromised IoT devices effectively. In contrast to prior work, DİoT uses a novel self-learning approach to classify devices into *device types* and build normal communication profiles for each of these that can subsequently be used to detect anomalous deviations in communication patterns. DİoT is completely autonomous and can be trained in a distributed crowdsourced manner without requiring human intervention or labeled training data. Consequently, DİoT can cope with the emergence of new device types as well as new attacks. By systematic experiments using more than 30 off-the-shelf IoT devices, we show that DİoT is effective (94% detection rate) and fast (≈ 2 s.) at detecting devices compromised by the infamous Mirai malware. DİoT reported *no false alarms* when evaluated in a real-world deployment setting.

Keywords

IoT security; anomaly detection; intrusion detection; device type identification; smart home; self-learning security

1. INTRODUCTION

The growing popularity of the Internet-of-Things (IoT) has led to many new device manufacturers entering the IoT device market. The “rush-to-market” mentality of manufacturers leads to poor product design practices that leaves thorough security considerations often merely an afterthought. This has led to many devices being released with security vulnerabilities that can be exploited through various attacks. An entirely new category of malware has emerged [1, 15, 27,

47] explicitly targeting IoT devices, as these are increasingly popular and relatively easy to compromise.

The preferred way to cope with security vulnerabilities is to apply security patches through software and firmware updates on affected devices. However, some devices may lack appropriate facilities for automated updates or there may be significant delays until device manufacturers provide them. Another approach for protecting IoT networks is to deploy an intrusion detection system (IDS) that looks for *signatures* of known attacks. Such systems are ineffective at detecting novel attacks for which they do not yet have signatures. A network remains unprotected until the IDS vendor releases updated attack signatures covering the new attacks, which might incur significant delays.

A complementary approach is *anomaly detection* in which a pre-trained model of benign network traffic patterns is used to identify anomalous behavior since it is potentially malicious. However, the enormous fragmentation of the IoT device market makes traditional anomaly detection approaches infeasible. To be effective, an anomaly detection model requires capturing *all* benign patterns of behavior in order to differentiate benign from malicious behavior. Given the ever-increasing number of literally thousands of types of IoT devices (ranging from temperature sensors and smart light bulbs to big appliances like washing machines) an all-encompassing behavior model would be 1) tedious to learn and update, and 2) too broad to be effective at detecting subtle anomalies.

Goals and Contributions. Our goal is to develop a system for detecting compromised IoT devices that is effective without suffering from the deficiencies discussed above. We propose a novel approach that combines *automated device-type identification* and subsequent *device-type-specific anomaly detection* by making use of machine learning techniques. Using this approach, we demonstrate that we can effectively and quickly detect compromised IoT devices with few false alarms, an important consideration for deployability and usability of any anomaly detection approach. Major IoT device vendors, including CISCO, helped us formulate the setting for our solution and potential usage scenarios.

IoT devices like smart home appliances have limited functionality compared to general-purpose computing devices

like PCs and smartphones. Consequently, communication traffic involving IoT devices have more predictable and static behavior patterns. Hypothesizing that the communication characteristics of a compromised IoT device will deviate sufficiently from a clean device, we propose a novel approach for detecting compromised IoT devices. Our approach is based on building models of normal (benign) communication behavior for classes of IoT devices grouped according to *device types*. Unlike previous approaches [34, 39, 40], device types and their normal communication profiles are learned *automatically*, requiring no human intervention or labeling of any training data. Both device-type identification and anomaly detection models are trained in a distributed manner using unlabeled crowdsourced data.

We make the following contributions:

- D \ddot{I} oT, a self-learning distributed system for security monitoring of IoT devices (Sect. 3)
- a novel self-learning identification method based on passive fingerprinting of periodic communication traffic of IoT devices (Sect. 4). In contrast to previous methods, it requires *no prior knowledge* about device types nor labeled training data and is effective at identifying the type of an IoT device in *any state of a device’s operation*. Using a large dataset comprising 33 typical real-world IoT devices, we show that our method achieves 98.2% accuracy.
- a novel GRU (gated recurrent unit)-based anomaly detection approach representing network *packet sequences as strings in a language* and leveraging *device-type-specific detection models* (Sect.5). It detects compromised IoT devices quickly (≈ 2 s.) and accurately (success rate of 94%), *without raising any false alarm* during one week of evaluation in a real-world deployment setting.
- an *attack dataset* of network traffic generated by real off-the-shelf consumer IoT devices infected with real IoT malware (Mirai [1]) using which we evaluate the effectiveness of D \ddot{I} oT (Sect.6).

We will make our datasets as well as the D \ddot{I} oT implementation available for research use.

2. PRELIMINARIES

2.1 IoT Malware

Recently, a number of large-scale attacks utilizing vulnerabilities in IoT devices have been widely reported in news reports. The Mirai malware [1] is the most well-known, which targeted specifically IoT devices having basic security flaws [29, 27]. Subsequently other similar malware attacks like Persirai [62], Hajime [15] and BrickerBot [47] have emerged. Pa *et al.* [43] identified that IoT malware attacks can be divided into three stages: *intrusion, infection and monetization*. The intrusion stage utilizes weaknesses like default administrator or root passwords, or exploits of known vulnerabilities in particular IoT devices to gain unauthorized access to devices. In the infection stage, attackers upload a piece of malicious code to the device and execute it. In the monetization phase the malware typically performs network scans for identifying other vulnerable devices causing also these devices to get infected. Finally, the malware takes malicious actions like acting as part of a bot network for distributed denial of service (DDoS) attacks (e.g., in the case of Mirai [27]). Other monetization methods may in-

clude unauthorized leakage of information from the user’s network to outsiders.

2.2 Device-Type Identification

Earlier device-type identification schemes have the primary goal of using various device fingerprinting approaches for identifying either the device model [40] or the specific hardware / software configuration of a device [26, 7, 17, 6] by training classification models with *labeled data* from specific known device types. Such training data requires extensive human effort to generate and maintain.

D \ddot{I} oT takes a different approach: the purpose of identification in D \ddot{I} oT is to enable efficient anomaly detection. Hence, there is no need to identify the real-world model of each device. It is sufficient to reliably map devices to a “device type” for which the system can build a model of normal behavior that can be used to effectively detect anomalous deviations. Therefore D \ddot{I} oT can be trained without the need to manually label the communication traces of pre-defined real-world device types. Rather, a clustering algorithm is used to identify *abstract device types* (cf. Sect. 4) to which devices are mapped based on their observed communication behavior. The training and evaluation of the anomaly detection models (cf. Sect. 5) are performed in terms of these abstract device types. This allows D \ddot{I} oT to be trained and operated autonomously, *without the need for human intervention at any stage*.

3. SYSTEM MODEL

Our system model is shown in Fig. 1. We consider a typical SOHO (Small Office and Home) network, where IoT devices connect to the Internet via an access gateway.

3.1 Adversary Model

Our adversary is a typical IoT malware botnet that actively scans for vulnerable devices in the SOHO network and infects vulnerable devices found by uploading and executing malware code on the compromised devices. Once compromised, IoT devices take malicious actions as described in Sect. 2.1. Typically adversary botnets use two different kinds of active components: botnet servers and infected IoT devices (both local and remote). Botnet servers can assume different roles. In the case of Mirai the *command & control* server directs the actions of infected IoT devices, the *loader* server infects vulnerable devices by uploading malware code onto them, and the *listener* server harvests scanning reports of potentially vulnerable devices, sent to it by infected IoT devices belonging to the botnet.

The primary goal of D \ddot{I} oT is to *detect infected IoT devices on the local network* in order to be able to take appropriate countermeasures against them, e.g., by isolating them from the rest of the network. Countermeasures against remote adversaries are outside the scope of D \ddot{I} oT, as we don’t assume to have any control whatsoever over remote hosts on the Internet (other than potentially notifying responsible authorities about IP addresses associated with the adversary).

3.2 Challenges and Assumptions

Anomaly detection techniques can automatically identify infected devices. However, in the IoT application scenario, it faces some challenges:

- **C1 - Dynamic threat landscape.** New IoT devices are released on a daily basis. A significant sub-

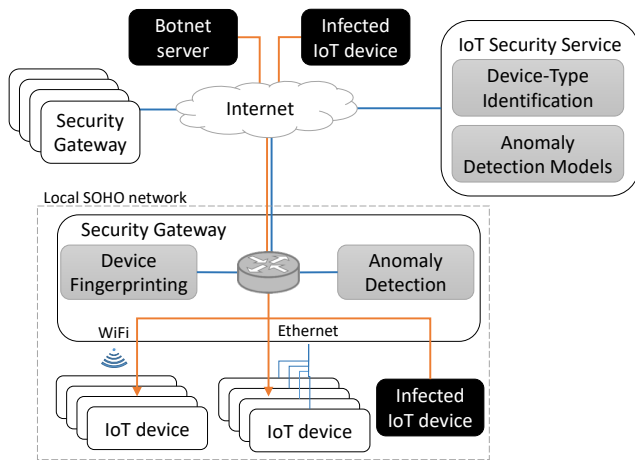


Figure 1: DIoT system model

set of them have security vulnerabilities. Exploits targeting vulnerable devices are also being developed by adversaries at a similarly high pace. This makes the threats against IoT devices highly dynamic and ever-increasing.

- **C2 - Resource limitations.** IoT devices have limited capabilities w.r.t. available memory, computing resources and energy making it infeasible to perform on-device detection in many cases.
- **C3 - IoT device heterogeneity.** IoT device types are very heterogeneous but individual devices are relatively limited in terms of functionality and processes they run. Consequently, the network traffic different device types generate is clearly different from each other.
- **C4 - Scarcity of communications.** In contrast to high-end devices, IoT devices generate only little traffic, often triggered by infrequent user interactions.
- **C5 - False alarms.** Anomaly detection techniques easily raise many false alarms. To be useful in practice, the systems must seek to minimize such false alarms.

We make the following assumptions regarding the vulnerabilities and infection of IoT devices:

- **A1 - Delay to exploit vulnerability.** IoT devices may be vulnerable but are not compromised when first released by a manufacturer. Adversaries must first obtain a device to find a vulnerability and a way to exploit it. This process takes a few days during which non-compromised devices of a given type are deployed and generate only legitimate communications.
- **A2 - Installation of non-compromised devices.** IoT devices are not compromised when first installed to a SOHO network. They remain uncompromised several hours before an adversary can find and compromise them.

3.3 System Design

3.3.1 Design Choices

Gateway monitoring: We detect compromised IoT devices by monitoring their communication as observed by Security Gateway that acts as a gateway for the local network. All IoT devices are directly or indirectly connected

to this gateway, which observes all external communications to the Internet as well as most local device-to-device communications. It represents an extensive and unconstrained monitoring point, effectively addressing challenge **C2**.

Device-type-specific anomaly detection: Since IoT devices have heterogeneous behavior (challenge **C3**), we model each device-type’s legitimate behavior with a dedicated model. Consequently, each anomaly detection model captures a relatively homogeneous and limited behavior, representing a single device type. This approach leads to a restrained model that is able to capture all possible legitimate behaviors of a device type. Thus the model is expected to be more sensitive to subtle anomalies, increasing its detection capability, and less prone to trigger false alarms. This design choice partially addresses challenge **C5**.

Autonomous self-learning system: DIoT learns anomaly detection profiles using data samples that only have labels telling which device types generated them. These labels representing individual device types are automatically generated and assigned. This is done by building fingerprints for the communication patterns of each IoT device. DIoT uses an unsupervised machine learning approach to cluster these fingerprints and autonomously create a label for each cluster representing a device type (device-type identification in Sect. 4). The whole process does not require any human intervention, which allows DIoT to respond quickly and autonomously to new threats, addressing challenge **C1**. It is worth noting that DIoT starts operating with no device-type identification or anomaly detection model. It learns and improves these models as Security Gateways aggregate more data.

Information aggregation: Information gathered by different Security Gateways is correlated in a central entity, the IoT Security Service. Anomaly detection models are learned using a *federated learning approach* where Security Gateways use locally collected data and collaborate with IoT Security Service to train the models (details in Sect. 5.3). IoT Security Service similarly uses fingerprints generated at several Security Gateways to learn device-type identification models (details in Sect. 4.3). This aggregation maximizes the usage of limited information obtained from scarce communications at each gateway (challenge **C4**). It is also expected to improve the accuracy of anomaly detection models (challenge **C5**) by learning from the maximum amount of data available.

Modeling techniques requiring little data: As later presented in Sect. 4 and 5, we define features and select machine learning algorithms that work with few training data for both device-type identification and anomaly detection. This design choice addresses challenge **C4**.

3.3.2 System architecture

The DIoT system consists of Security Gateway and IoT Security Service. The role of Security Gateway is to monitor devices and perform device fingerprinting and anomaly detection in order to identify compromised devices in the network. It is supported by IoT Security Service that performs device-type identification based on the fingerprints provided and aggregates device-type-specific anomaly detection models used by Security Gateway.

Security Gateway acts as the local access gateway to the Internet to which IoT devices connect over WiFi or an Ethernet connection. Apart from acting as a gateway router

for connected devices in the local network, Security Gateway hosts two functions: the Device Fingerprinting and Anomaly Detection components. The task of Device Fingerprinting is to monitor the communication patterns of connected IoT devices and extract *device fingerprints* for identifying the device type of the connected device (details in Sect. 4). Device Fingerprinting is a one-time operation that is performed when a new IoT device is detected in the network. An identified device is assigned to its corresponding type which it retains permanently unless fingerprinting is re-initiated, e.g., due to a detected firmware update on the device (cf. Sect. 8). The Anomaly Detection component continuously monitors the communications of identified IoT devices and detects devices displaying abnormal communication behavior that is potentially caused by malware (details in Sect. 5). Security Gateway also provides locally collected data to IoT Security Service for learning device-type identification and anomaly detection models.

IoT Security Service supports Security Gateway. It is a cloud-based functionality hosting two main components: Device-Type Identification and Anomaly Detection Model. Device-Type Identification uses a machine learning-based classifier for *identifying the device type of IoT devices* based on device fingerprints provided by Security Gateway. Anomaly Detection Model maintains a repository of device-type-specific *anomaly detection models*. After successful identification of a device’s type, IoT Security Service sends the identified device type and corresponding anomaly detection model to Security Gateway. Upon receiving the anomaly detection model for the type of an identified IoT device, Security Gateway starts monitoring its communications in order to detect potential deviations from normal behavior encoded by the detection model.

4. DEVICE-TYPE IDENTIFICATION

Traditional device-type identification approaches [34, 46] rely on aggregated statistics extracted from dense network traffic. These are ineffective when applied to IoT devices due to the scarcity of their communication (cf. Sect. 3.2 - challenge C4). IoT devices generate little dense traffic, typically only during rare and short user interactions. Nevertheless, IoT devices also generate background communication independent of user interactions. This traffic is always present, relatively constant and periodic. Thus, we introduce a novel technique for identifying the type of IoT devices based on their periodic background network traffic. In contrast to existing approaches, this technique can identify the type of an IoT device *in any state of operation*, including standby, with a constant time of 30 minutes. Our technique is composed of three steps relying on passive monitoring of the network traffic at the network gateway: step 1: inference of periodic flows, their period and stability (Sect. 4.1), step 2: extraction of a fingerprint characterizing a device-type based on its periodic flows (Sect. 4.2) and step 3: use of this fingerprint in a supervised classification system that identifies device-types (Sect. 4.3). The overview of the identification process is depicted in Figure 2. Steps 1 and 2 are implemented in Security Gateway while step 3 is implemented in IoT Security Service.

4.1 Periodic Flow Inference

The first step in our device-type identification technique is to infer the periodicity in the communication of a device.

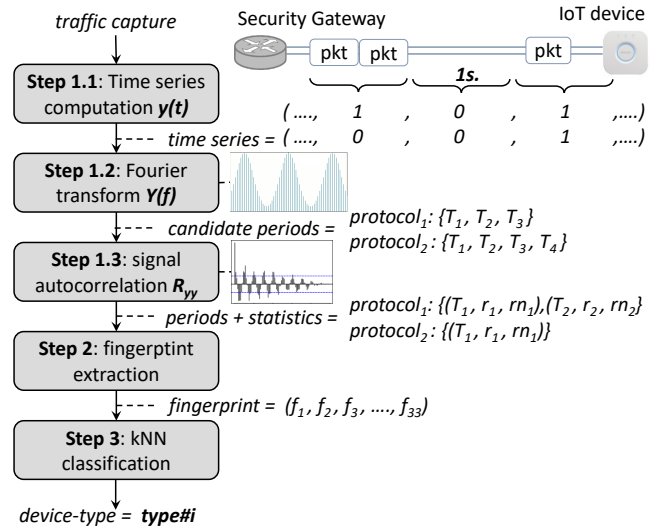


Figure 2: Overview of device-type identification.

Fourier transform and signal autocorrelation are effective signal processing techniques for inferring periodicity. We divide the network traffic of a device into distinct flows and apply these techniques to the flows.

Several non-IoT devices and processes are running in a typical smart home IoT network. Most of them do not generate periodic traffic. While Fourier transform and signal autocorrelation can identify the several distinct periods of a signal, ignoring most non-periodic noise, these techniques are more accurate when applied to pure single-periodic signals. As a result, we pre-process the network traffic received at Security Gateway and divide it into distinct *flows* that can expose none, one or a small number of periods. In this context, we define a *flow* as a sequence of network packets sent from a given source MAC address (IoT device) using a given communication protocol (e.g., NTP, ARP, RTSP, etc.). The rationale for flow division is that most periodic communication uses dedicated protocols that are different from the ones used for communication related to user interaction (non-periodic). If periodic and non-periodic communication still coexist in a flow (e.g., HTTP), Fourier Transform and signal autocorrelation can cope better with this reduced non-periodic noise.

The flow of packets in a network capture must be converted into a format suitable for signal processing. We discretize each flow into a binary time series sampled at one value per second, indicating whether the flow contained one or more packets during the 1-second period (value 1) or not (value 0). The computed time series is a discrete binary signal $y(t)$ of duration d seconds.

We first use the discrete Fourier transform (DFT) [60] to identify candidate periods for a given flow. The DFT converts a discrete signal $y(t)$ from the time domain to the frequency domain: $y(t) \Rightarrow Y(f)$. $Y(f)$ provides amplitude values for each frequency $f \in [0, 1]$. The frequency f_i resulting in the largest amplitude $Y(f_i) = \max(Y(f))$ gives the periodicity $T_i = \frac{d}{f_i}$ of the dominant period in $y(t)$. Secondary periods T_j of lower amplitude also exist. We select candidate periods T_i having an amplitude $Y(\frac{d}{T_i})$ larger than 10% of the maximum amplitude $\max(Y(f))$. We discard close

candidate periods by selecting only local maxima of $Y(f)$. The result of this operation is a list of candidate periods for a flow.

Candidate periods found using DFT can be nonexistent or inaccurate. To confirm and refine these periods, we compute the discrete autocorrelation R_{yy} of $y(t)$. R_{yy} denotes the similarity of the signal $y(t)$ with itself as a function of different time offsets. If the autocorrelation R_{yy} at offset l is large and reaches a local maximum, it means that $y(t)$ is likely periodic, with period $T = l$ and that this period occurs $R_{yy}(l)$ times over $y(t)$. For each candidate period T_i obtained with DFT, we confirm and refine it by analyzing the value of $R_{yy}(l_i)$ on the range of close offsets $l_i \in [0.9 \times T_i; 1.1 \times T_i]$. If it contains a local maximum $R_{yy}(l_i) = \text{lm}ax_i$, we confirm the existence of a period that belongs to this range and update its value to $T_i = l_i$. For each resulting period T_i we compute characteristic metrics r_i and rn_i , defined in Equation (1) and (2) respectively.

$$r_i = \frac{T_i \times R_{yy}(T_i)}{d} \quad (1)$$

$$rn_i = \frac{T_i \times (R_{yy}(T_i - 1) + R_{yy}(T_i) + R_{yy}(T_i + 1))}{d} \quad (2)$$

r_i computes the ratio of occurrences of period T_i over signal $y(t)$ of duration d seconds. An accurate and stable periodic signal of period T_i renders $r_i = 1$. However, a periodic signal may be noisy ($r_i < 1$) or have parallel periods of same periodicity. Periodic signals may also be unstable and present slight differences in their periodicity ($r_i < 1$). This is the rationale for computing rn where we sum the occurrences of neighboring periods $R_{yy}(T_i - 1)$, $R_{yy}(T_i)$ and $R_{yy}(T_i + 1)$. A stable signal of period T_i produces $r_i \approx rn_i \approx 1$, while unstable signals produce $r_i < 1$ and $r_i \ll rn_i$.

The final result of period inference for a flow is a set of periods with the corresponding ratios r_i and rn_i : $\{(T_1, r_1, rn_1), \dots, (T_n, r_n, rn_n)\}$. An example of periodic flow inference is provided in Appendix A.

4.2 Fingerprint Extraction

Having inferred periodic flows of an IoT device, we want to identify its *type*. We build a fingerprint for a device type by extracting features from results obtained from periodic flow inference. This fingerprint is a feature vector of 33 features.

We split a network traffic capture of x seconds into three sub-captures $[0; \frac{x}{2}]$, $[\frac{x}{4}, \frac{3x}{4}]$, $[\frac{x}{2}, x]$. We apply periodic flow inference (Sect. 4.1) on each sub-capture and on the whole capture $[0; x]$. We obtain four sets of periods with the metrics r and rn for each flow. The goal of applying period inference on smaller sub-captures is twofold. First, we obtain more significant results by discarding periods that are inferred from less than two sub-captures. Second, we can compute statistics from metrics r and rn to measure their stability.

The results from period inference are grouped by source MAC address, which is linked to a single device. This grouping defines the granularity of feature extraction, i.e., one fingerprint is extracted per source MAC address and capture. We introduce 33 features that compose our device-type fingerprint. These features are manually designed to model a group of periodic flows in a unique manner that enables to distinguish device types. There are four categories of fea-

tures as discussed below. A detailed feature description is presented in Tab. 5 in Appendix B.

Periodic flows (9 features). This feature category characterizes the quantity and quality of periodic flows. It includes the count of periodic flows (1), the layer of protocols that support periodic flows (2), if flows are single- or multi-periodic (3-6), if there is a change in the source port of periodic flows (7) and the frequency of this change (8-9).

Period accuracy (3 features). These features measure the accuracy of the inferred periods and characterises how noisy the flows they were extracted from are. They consist of the count of periods that were inferred from all sub-captures and the whole capture (10), the mean (11) and standard deviation (12) for the count of sub-captures from which each period was inferred.

Period duration (4 features). These features (13-16) represent the number of periods that belong to four duration ranges, e.g., [5s.; 29s.]. The ranges were manually chosen in an attempt to segregate periods according to their relative duration: [5s.; 29s.]; [30s.; 59s.]; [60s.; 119s.]; [120s.; 600s.]. Short durations are allocated to smaller ranges than long durations. Periods of less than 5 seconds or more than 10 minutes are discarded. Identifying long periods requires long traffic captures which slows down the fingerprint extraction.

Period stability (17 features). Features in this category measure the stability of the inferred periods using r and rn metrics, as discussed in Sect 4.1. The mean and standard deviation (SD) of r and rn metrics are computed for each flow and period. Features 17-20, respectively 24-27, are calculated by binning the values of $\text{Mean}(r)$, respectively $\text{Mean}(rn)$, into four ranges and counting the number of values in each bin. The bin ranges of mean r and rn values were selected to distinguish noisy [0.2; 0.7[from pure [0.7; 1[single-period flows as well as different multi-periodic flows [1; 2[, [2; +∞[. Features 21-23, respectively 28-30, are calculated by binning the values of $\text{SD}(r)$, respectively $\text{SD}(rn)$, into three ranges and counting the number of values in each bin. These ranges were selected to distinguish very stable [0; 0.02[from stable [0.02; 0.1[and unstable [0.1; +∞[periodic flows. Features 31-33 are computed by binning the values of the difference $rn - r$ and into three ranges of values and counting the corresponding bin cardinalities. These ranges were selected to characterize the differences between stable and unstable periods of flows.

4.3 Device-Type Fingerprint Classification

Our device-type identification technique is designed to be fully autonomous. It doesn't require human interaction nor labeled data to operate. When an IoT device is associated to a Security Gateway, the latter monitors its network traffic and extracts a fingerprint as described in Sect. 4.2. It is sent to the IoT Security Service, which attempts to identify the type of the device having this fingerprint. If the fingerprint has a match, the type of the device is identified and the fingerprint is used to retrain and improve its identification model. If no match is found, the IoT Security Service does not have an identification model for this device type yet. It uses the unidentified fingerprints to learn a model for this new device type.

As mentioned earlier, device types we use here are abstract. They do not refer to meaningful pre-learned labels such as "*D-LinkCam IP camera*" but are reference identifiers specific to D-IoT, e.g., *type#12*. These identifiers match be-

havior models used for anomaly detection as later presented in Section 5.

The system starts operating with no identification model. As IoT Security Service receives fingerprints from Security Gateway, it creates type identifiers (e.g., *type#12*) and learns an identification model for them. The longer the system runs and the more Security Gateways contribute to it, the more device types it is able to identify and the better the accuracy of identification is.

We implement the automated device-type identification using a supervised k-Nearest Neighbors (kNN) classifier [51]. kNN is chosen because of its ability to deal with a large number of classes and an imbalanced dataset. Each device type is represented by one class and the training data available for each class may be imbalanced (as IoT devices are differently deployed). kNN forms small clusters of at least k neighbors to represent a class. In supervised classification mode, several clusters can define a class, capturing its potential diversity. When fingerprints for device types unknown to the model are processed, they are detected as exceeding a threshold distance to the nearest cluster of the classification model. A new class can be added to the model to represent this yet unknown device type.

Our features are processed and should not require complex association to differentiate device types. Thus, we use the simple Euclidian distance as distance measure in kNN. All 33 features of our fingerprints are scaled on the range [0; 1] to have an equal weight in the classification task. Fingerprints are extracted from network traffic captures of 30 minutes. We assessed empirically that 30 minutes provides the best trade-off between accuracy and speed of identification, i.e., considering longer captures does not improve accuracy. We set the minimum number of neighbors to define a class to $k = 5$ to meet a trade-off between representativeness of a learned class and need for training data. A class for a new device-type can be learned as soon as we get five fingerprints for it, i.e., after 2.5 hours of monitoring.

5. DEVICE-TYPE-SPECIFIC ANOMALY DETECTION

As discussed in Sect. 2.1, IoT malware typically affects the behavior of IoT devices through the activities it performs. It generates a significant amount of communications when performing the intrusion, infection and monetization [27] associated with the attack. Since these actions are not related to the normal functions of the device, they will generate new, previously unknown traffic patterns. Our goal is to detect whether or not the current traffic pattern matches the normal pattern and trigger an anomaly, if it doesn't.

In our approach, packet flows $\langle pkt_1, pkt_2, \dots, pkt_n \rangle$ present in normal, benign traffic generated by an IoT device are transformed into sequences of symbols $\langle s_1, s_2, \dots, s_n \rangle$ in which packets pkt_i of the flow are mapped to individual symbols s_i based on certain distinct characteristics present in each packet as discussed in Sect. 5.1. A neural network is then trained using these symbol sequences to form a model representing the inherent packet sequence patterns in benign packet flows. For this we employ Gated Recurrent Units (GRUs) [24, 11], a novel approach to recurrent neural networks (RNN) currently being a target of lively research. The GRU model will learn the normal sequences of packets present in the communication patterns of the considered

device type. To detect abnormal traffic patterns, we feed the symbols representing incoming packet flows to the GRU and obtain estimates for the occurrence probability of each new packet given the preceding sequence of packets. If the occurrence probability estimates p_i of a sufficient number of consecutive packets fall below a detection threshold, as described in detail in Sect. 5.2, it is deemed anomalous and an alarm is raised.

GRUs are a good compromise as they are able to accommodate more complicated (longer) communication patterns in comparison to, e.g., finite state automata. At the same time they can provide useful results without requiring very large datasets for training as discussed in Sect. 6.3, thereby addressing challenges C4 and C5.

5.1 Modelling Packet Flows

Data packets pkt_i are mapped into symbols $s_i = (c_1, c_2, \dots, c_7)$, which are 7-tuples of discrete values for packet characteristics presented in Tab. 1. This mapping is defined by a device-type-specific mapping function $pkt_i \rightarrow mapping_{type\#k}(pkt_i) = s_i A \rightarrow B_{type\#k}$, where A is the domain of raw network packets pkt and $B_{type\#k}$ is the domain of packet symbols s for device-type $type\#k$. It is worth noting that $B_{type\#k}$ is different for different device types.

Table 1: Packet characteristics used in symbol mapping

ID	Characteristic	Value
c_1	direction	incoming, outgoing
c_2	local port type	bin index of port type
c_3	remote port type	bin index of port type
c_4	packet length	bin index of packet length
c_5	TCP flags	TCP flag values
c_6	protocols	encapsulated protocol types
c_7	IAT bin	bin index of packet inter-arrival time

Characteristic c_1 is a binary value encoding the direction of each analyzed packet. Characteristics c_2 and c_3 encode the particular port types of local (IoT device) and remote port numbers, whereas c_4 is the bin index of the packet length. The binning is performed by assigning dedicated bins for the eight most frequently occurring packet lengths in the training data and assigning a ninth bin for all other packet lengths. Characteristics c_5 and c_6 encode the *TCP flag values* and the *encapsulated protocol types*, respectively. Characteristic c_7 is the bin index of three packet inter-arrival time (IAT) bins (<0.001ms, 0.001ms to 0.05ms, and > 0.05 ms).

Using the symbolic representations of the packet flows for each device of type $type\#k$, a GRU-based detection model is trained for $type\#k$ by feeding the symbol sequence as training data to it.

5.2 Detection Process

Using the trained GRU-based models for different device types, Security Gateway will perform anomaly detection on the incoming packet flow of each of the identified IoT devices connected to it, utilizing the detection model corresponding to each device's type. The data packet flow is transformed into its corresponding symbol sequence as discussed above and then sequentially fed to the detection model. For each symbol s_i of the sequence, the detection model will output an *occurrence probability* p_i of observing the cur-

rent symbol s_i given the sequence of k preceding symbols $\langle s_{i-k}, s_{i-k+1}, \dots, s_{i-1} \rangle$, i.e.,

$$p_i = P(s_i | \langle s_{i-k}, s_{i-k+1}, \dots, s_{i-1} \rangle) \quad (3)$$

The parameter k is a property of the used GRU network and denotes the length of the lookback history, i.e., the number of preceding symbols that the GRU takes into account when calculating probability estimates for the possible next symbols in the symbol sequence. In effect, the GRU model will provide for each packet in the observed sequence of incoming packets an estimate of how probable the occurrence of this packet is given the preceding sequence of packets. We postulate that these probability estimates will be on average higher for known benign traffic patterns, while traffic patterns generated as a result of malware on an infected device will be lower and can therefore be flagged as anomalous. We therefore define anomaly criteria for triggering a detection as follows.

We define a packet to be *anomalous*, if the occurrence probability of the symbol corresponding to it is below a pre-defined *detection threshold* δ :

DEFINITION 1 (ANOMALOUS PACKETS). *A packet pkt_i represented by symbol s_i is anomalous, if its occurrence probability p_i is below the detection threshold δ , i.e., if*

$$p_i < \delta \quad (4)$$

A special challenge in our case is that the network traces of infected devices typically contain both benign *and* malicious traffic. The benign traffic is caused by the continued 'normal' operations of the device in question, while the malicious traffic is caused by actions of the malware executing on the infected device. However, if we would trigger an anomaly each time an anomalous packet is observed, this would lead to numerous false positive detections, as benign traffic also contains systemic noise that is not captured by the GRU detection model and will therefore receive low occurrence probability estimates. We therefore aggregate the detection results over several consecutive packets and trigger an anomaly only in the case that a significant number of consecutive packets are anomalous.

DEFINITION 2 (ANOMALY TRIGGERING CONDITION). *Given a window W of w consecutive packets $W = \langle pkt_1, pkt_2, \dots, pkt_w \rangle$ represented by symbol sequence $S = \{s_1, s_2, \dots, s_w\}$, we trigger an anomaly alarm, if the fraction of anomalous packets in W is larger than an anomaly triggering threshold γ , i.e., if*

$$\frac{|\{s_i \in S | p_i < \delta\}|}{w} > \gamma \quad (5)$$

5.3 Federated Learning Approach

Our GRU models are learned using traffic collected at several Security Gateways, each monitoring a client IoT network. Each Security Gateway observing a device of type *type#k* contributes to training its anomaly detection model. We take a *federated learning* approach to implement the distributed learning of models from several clients. Federated learning is a communication efficient and privacy preserving learning approach suited for distributed optimization of Deep Neural Networks (DNN) [28, 55]. In federated learning, clients do not share their training data but rather train a local model with it and send reports of model modification

to a centralized entity which aggregates them. Federated learning is chosen because it is suitable [38] for scenarios where:

- the training data are user dependent, i.e., data coming from one user may not be representative of the whole population distribution. This is the case for IoT device communication, which depends on user interaction and differs between users.
- the data are massively distributed, meaning that a large number of clients participate and each has a small amount of data. IoT devices typically generate little traffic, which means only little training data can be provided by each client alone.
- the contribution from each client is imbalanced. In our system, the training data available at each Security Gateway depends on the duration that an IoT device has been in the network and the amount of interaction it has had. This varies largely from one client to the other.

Each Security Gateway reporting to have a *type#k* device in its network gets a base global GRU model from IoT Security Service. At the start of D^IOT, this model is random, otherwise it is already trained through several rounds of the following process. The global model is re-trained locally by each Security Gateway with traces collected by monitoring communication of the *type#k* device. Local updates made to the model by each Security Gateway are reported to IoT Security Service which aggregates them to improve the global model. The updated global model for *type#k* devices is then pushed back to Security Gateway and used for anomaly detection. The re-training of the model is performed on a regular basis to improve anomaly detection.

Federated learning is a well studied research topic. Several generic solutions have been proposed and evaluated [28, 23, 55], which can implement in a straightforward manner our federated learning model for GRU. Consequently, we do not evaluate it in this paper.

6. EVALUATION

6.1 Datasets

To evaluate our device-type identification and anomaly detection approaches, we collected extensive datasets the communication behavior of IoT devices in both a laboratory and a real-world deployment setting. The monitored devices included 33 typical consumer IoT devices like IP cameras, smart power plugs and light bulbs, sensors, etc. The detailed list of devices can be found in Tab. 7 in Appendix D.

6.1.1 Description

Background dataset. In order to identify the inherent communication patterns of IoT devices, we collected a dataset characterizing the background traffic IoT devices generate while no explicit actions are invoked. This dataset captures any communications resulting from actions devices execute in standby mode, like, e.g., heartbeat messages or regular status updates or notifications.

Activity dataset. A key characteristic of IoT devices is that they are typically single-purpose devices with inherently less diverse behavior than general-purpose computing devices like, e.g., desktop computers, tablets or smartphones. Most devices expose only a few distinct actions accessible to users, e.g., ON, OFF, ADJUST, etc. To cap-

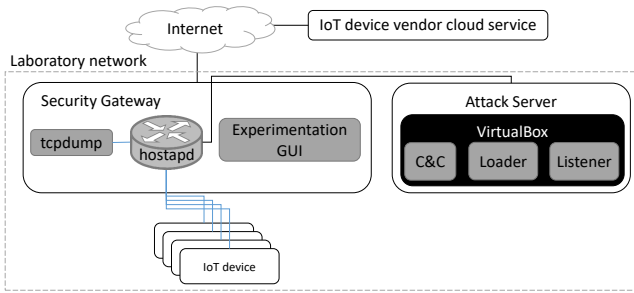


Figure 3: Lab network setup

ture the communication patterns related to user interactions with IoT devices, we collected a dataset encompassing all such actions being invoked on the respective IoT devices, in order to capture the full diversity of each IoT device’s user-activity-related behavior.

Attack dataset. For evaluating the effectiveness of our anomaly detection approach, we collected a dataset with attack traffic of IoT devices that we infected with the Mirai malware [27]. We selected Mirai, since its source code is publicly available. This enabled us to make modifications in the malware code that allowed us to separately examine malware traffic patterns when it is executing different kinds of attacks as discussed in detail in Sect. 6.3. Several malware variants like Persirai [62] or Hajime [15] have been implemented using the same code base or closely follow a similar behavior. This makes Mirai a relevant baseline for IoT malware behavior.

Deployment dataset. To evaluate the performance of D²IoT in a realistic deployment setting, in particular with regard to how many false alarms D²IoT can be expected to raise in a real smart home setting, we installed a number of (n=14) different smart home IoT devices in several different domestic deployment scenarios involving real users and collected communication traces of these devices under realistic usage conditions.

6.1.2 Data Collection

We performed data collection of the *background*, *activity* and *attack* datasets in a laboratory network as shown in Fig. 3, using a set-up that allowed us to capture all network traffic generated by the examined IoT devices. For this setup, we used `hostapd` on a laptop running Kali Linux to create a Security Gateway (SGW) acting as an access point with WiFi and Ethernet interfaces to which all IoT devices were connected. On the SGW we then collected network traffic packets originating from the devices using `tcpdump`, filtering out packets not related to the devices based on each device’s MAC address. The vast majority of the analyzed devices used either WiFi or Ethernet to connect to the user network. A number of devices like smart light bulbs or sensors, however, utilize low-energy protocols like ZigBee, Z-Wave or Bluetooth Low Energy (BLE) to connect. Nevertheless, all of these devices connect to the user network with the help of a hub device that is connected either over WiFi or Ethernet to the network. For these devices, we monitored therefore the indirect traffic between the hub device and our Security Gateway.

Background dataset. Background traffic was collected for 33 devices by configuring a number of devices to the

Table 2: Actions for different IoT device categories

Category (count)	Typical actions
IP cameras (6)	START / STOP video, adjust settings, reboot
Smart plugs (9)	ON, OFF, meter reading
Sensors (3)	trigger sensing action
Smart lights (4)	turn ON, turn OFF, adjust brightness
Actuators (1)	turn ON, turn OFF
Appliances (2)	turn ON, turn OFF, adjust settings
Routers (2)	browse amazon.com

laboratory network, verifying the correctness of the setup and then leaving the devices on their own for a period of at least 24 hours. During this time, no actions were triggered or interactions with the devices undertaken.

Activity dataset. Activity data was collected by connecting each IoT device to the laboratory network and repeatedly performing actions shown in Tab. 2 with the devices. Each of the actions was repeated 20 times, while leaving short pauses of random duration between individual actions. To capture also less intensive usage patterns, the dataset was augmented with longer measurements of two to three hours, during which actions were triggered only occasionally. The activity dataset contains data from 27 IoT devices, a subset of those used for collecting the background dataset, as some devices like above-mentioned hub devices for lighting or home automation do not provide meaningful actions that users could invoke.

Attack dataset. Traffic was collected from five devices infected with the Mirai malware: D-LinkCamDCS930L, D-LinkCamDCS932L, EdimaxPlug1101W, EdimaxPlug2101W and UbnTAirRouter. This was done by installing the **Command & Control**, **Loader** and **Listener** server modules on the laboratory network for controlling the infected IoT devices acting as bots. The devices were infected using a security vulnerability like an easy-to-guess default password to open a terminal session to the device and uploading and activating the malware binary on the device. Communication data of the compromised devices were then captured. To make sure that malicious traffic did not enter the public Internet, the SGW was configured to drop all attack traffic targeted at addresses outside the laboratory network.

To investigate the performance of our anomaly detection method, we tested it in two operational modes: scanning and attacking. In scanning mode, the scanning function of the malware was activated, which resulted in the infected device actively scanning for other vulnerable devices. We also tested the malware in attack mode, utilizing various attack vectors available in the Mirai source code [18]. We therefore prepared 10 different versions of the malware and ran each of them separately (for details, see App. F).

Deployment dataset. In the domestic deployment environments, a similar data collection set-up as in the laboratory network, however excluding the attack server, was installed in the test users’ home environment. To protect the privacy of the users, the studied IoT devices were separated in a dedicated WiFi network and data collection was strictly limited to the targeted devices. The users were encouraged to use and interact with the IoT devices as part of

Table 3: Characteristics of used datasets

Dataset	Size (MB)	Flows	Packets
Background	226	56,337	127,532
Activity	239	59,577	134,867
Deployment	796	99,901	1,323,200
Attack	716	1,552,858	1,552,858

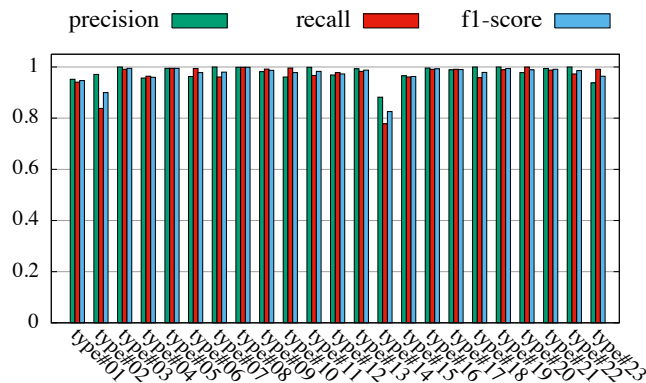


Figure 4: Precision, recall and f1-score for identification of 23 device types (e.g., *type#01*).

their everyday life. Packet traces originating from each of the devices were then collected during a monitoring period of one week.

Table 3 summarizes the sizes and numbers of distinct packets and packet flows contained in the different datasets used for our evaluation. While packet flows can’t be directly mapped to distinct device actions, they do, however, provide a rough estimate about the overall activity of the targeted devices in the dataset.

6.2 Device-Type Identification

To evaluate our device-type identification techniques, we computed fingerprints (cf. Sect. 4.2) from the *background* and *activity* traffic dataset. We obtained 6,224 fingerprints representing 33 IoT devices.

To assess the relevancy of our automatically defined device types, we trained a kNN model from the fingerprints, following the method presented in Sect. 4.3. It defined 23 classes each representing a device type. 16 devices were each assigned a single device type. 17 devices were aggregated into 7 classes. The assignment of IoT devices to self-defined device-types is summarized in App. C. Different devices identified to a given device type are always from same manufacturer and have a same or similar purpose (smart plugs / IP cameras / smart switches / sensors). For example, *type#06* contains two instances of the same IP camera. We conclude that our grouping is relevant for our anomaly detection system since similar/same devices from same manufacturers are likely to expose similar behavior that can be represented by a single anomaly detection model.

We demonstrate the accuracy of device-type identification using a 4-fold stratified cross-validation. We randomly split our 6,224 fingerprints in four equal subsets while respecting class (device type) distribution. We use three subsets for training our kNN identification model and test it on the remaining subset. This process is repeated four times to test each of the four subsets. We ran the cross-validation

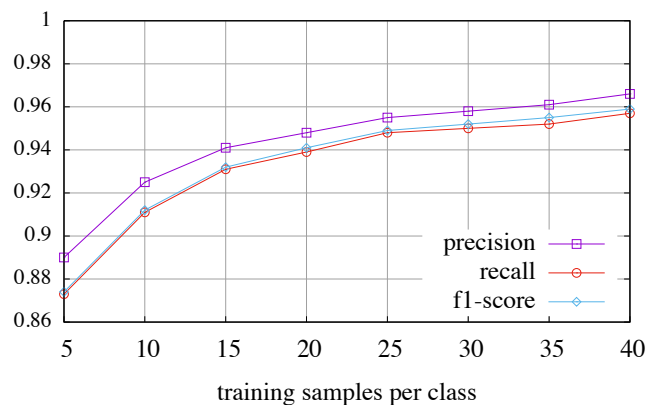


Figure 5: Precision, recall and f1-score increase with respect to training set size.

10 times with random seeds. Figure 4 presents the precision, recall and f1-score for identifying each device type. All metrics reach over 0.95 for most devices. The overall accuracy of identification across all types is 0.982, showing its effectiveness. A confusion matrix presents detailed results for this experiment in App. E.

To show that our identification model can be quickly learned, we evaluate its accuracy with a varying amount of training data. As presented in Sect. 4, we selected $k = 5$ as minimum number of components for a class in kNN. Figure 5 depicts the increase in precision, recall and f1-score as we vary the size of the training set from 5 fingerprints per device (2.5 hours monitoring) to 40 fingerprints per device (20 hours). We see that the accuracy in all metrics increases quickly from 0.87 to 0.95 but then stabilizes with a small gradient. It shows that after a few (≈ 12) hours of monitoring, more training data does not significantly increase accuracy. This time is likely even shorter considering that several **Security Gateways** contribute training data (fingerprints) for each device type in parallel. This shows that learning an effective device identification model requires only a few hours of traffic monitoring.

We evaluated our device-type identification technique on a large set of 33 IoT devices. We showed that our method for automatically learning device type is relevant. We demonstrate that the identification technique is effective and accurate, even when using little training data, which makes it fast at identifying newly released IoT devices.

6.3 Intrusion Detection

6.3.1 Evaluation Metrics

To evaluate the performance of our anomaly detection approach, we use the false positive and true positive rates (FPR and TPR) as measures of fitness. The FPR is a measure for how often benign communication is incorrectly classified as anomalous by our method, while the TPR measures reliability of reporting attacks as anomalous. We seek to minimize FPR while maximising TPR, since a high FPR negatively affects the usability of the system due to many false alarms. A high TPR on the other hand indicates that only few attacks remain undetected by the approach.

Testing for false positives was performed by four-fold cross-validation. We created two settings, a *lab setting* using the

union of the *background* and *activity* datasets, and a *deployment setting* using the *deployment* dataset. The *lab setting* is primarily used for parameters tuning of our anomaly detection approach (Sect. 5.2) and to select the best parameters to use in the *deployment setting*. Each setting is evaluated individually by dividing each of their respective datasets equally into four folds using three folds for training and the remaining fold for testing. To know the rate of false positives, we divided the testing dataset according to Def. 2 into windows of w packets. Since the testing data contained only benign communications, any triggered anomaly alarm for packets of the window indicated it as a false positive (FP), whereas windows without alarms were considered a true negative (TN).

Testing for true positives was done by using the *background* and *activity* datasets as training data and each of the different *attack* datasets for testing. As we know that the *attack* dataset also contains benign traffic corresponding to normal operations of IoT devices, we were interested in the average duration until detection. Therefore we divided the testing dataset into windows of w packets. In each window we calculated the number of packets required until an anomaly alarm was triggered in order to estimate average detection time. In terms of TPR, such windows were considered true positives (TP), whereas windows without triggered alarms were considered false negatives (FN). The resulting evaluation metrics were then calculated as follows:

$$TPR = \frac{TP}{TP + FN} \quad FPR = \frac{FP}{FP + TN} \quad (6)$$

6.3.2 Results

Based on initial experiments with our datasets (Table 4) we inferred that a lookback history of $k = 20$ symbols is sufficient to capture most communication interactions with sufficient accuracy. We used a GRU network with three hidden layers of size 128 neurons each. The size of the input and output layers is device-type-specific and equal to the number of mapping symbols of the function $mapping_{type\#k}$, which is equal to $|B_{type\#k}|$ (cf. Sect. 5.1). We learned 23 anomaly detection models, each corresponding to a device type identified in Sect. 6.2. Each anomaly detection model was trained with, and respectively tested on, communication from all devices matching the considered type (cf. Appendix C).

Table 4 shows the performance of our system for the different attack scenarios analyzed for the Mirai malware (cf. Sect. 6.1.2). The time to detect attacks varies according to the traffic intensity of the considered attack. Most aggressive DDoS attacks (and scanning) are detected in one second with 100% accuracy. The average detection delay over all tested attacks is 2.26 ± 4.69 seconds.

We evaluated FPR and TPR in the *lab setting* for different values of the detection threshold δ and anomaly triggering threshold γ using fixed $w = 250$. Figure 6 shows the ROC curve of FPR and TPR in dependence of these parameters. We can see that all curves increase very fast, reaching over 0.9 TPR while keeping a very low FPR < 0.01 . This was the objective for our anomaly detection system. We consider that an optimal performance is obtained for the values $\delta = 0.01$ and $w = 250$ for anomaly triggering threshold $\gamma = 0.5$, achieving 94.01% TPR for 0.8% FPR in the *lab setting*.

Using these selected parameters in the *deployment settings* provided the same attack detection rate of 94.01% TPR and

Table 4: Average detection times of analyzed Mirai attacks

Attack	packets/s.	det. time (s.)	TPR
scanning	292.18	0.43	100.00%
udp	84.44	1.72	100.00%
syn	752.60	0.17	100.00%
ack	123.83	1.09	94.56%
udpplain	1755.77	0.08	82.22%
vse	331.07	0.45	63.33%
dns	1292.56	0.10	100.00%
greip	167.84	0.75	100.00%
greeth	53.36	2.34	100.00%
http	10.92	15.43	100.00%

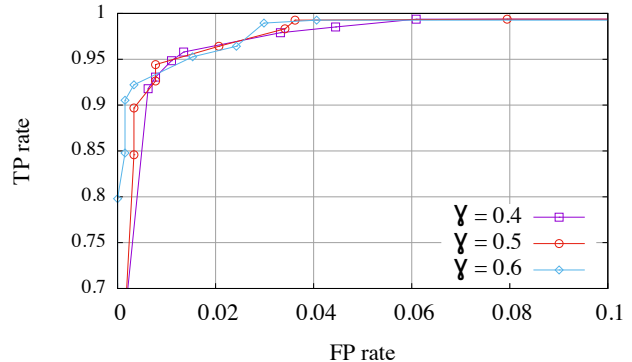


Figure 6: ROC curve of TPR and FPR in dependence of detection threshold δ and anomaly triggering threshold γ .

no false positives, i.e. 0% FPR during one week of evaluation. These results show that D \ddot{I} O \ddot{T} addresses challenge **C5**, reporting no false alarms in real-world deployment settings.

6.3.3 Performance

We evaluated processing performance of the GRU without specific performance optimizations on a laptop and a desktop computers. The laptop run Ubuntu Linux 16.04 with an Intel $\text{\textcircled{C}}$ Core TM i7-4600 CPU with 8GB of memory, whereas the desktop run Ubuntu Linux 18.04 with an Intel $\text{\textcircled{C}}$ Core TM i7-7700 CPU with 8GB of memory and a Radeon RX 460 core graphic card. Average processing time per symbol (packet) for prediction was $0.081(\pm 0.001)ms$ for the desktop with GPU and $0.592(\pm 0.001)ms$ when executed on the laptop with CPU. On average, training GRU models for each device type took 26 minutes on the desktop and 71 minutes on the laptop hardware when considering a week’s worth of data in the deployment dataset. We conclude from this that model training will be easily realizable in real deployment scenarios, as training will in any case be done gradually as data are collected from the network over longer periods of time.

7. SECURITY ANALYSIS

Knowing the design of D \ddot{I} O \ddot{T} , an adversary can try to circumvent anomaly detection.

Spoofing device fingerprint. A compromised device can attempt to modify its background traffic such that its fingerprint changes and it gets identified as another device type. This is unlikely to happen since fingerprinting is a one time

operation performed when a new IoT device is detected in the network. According to assumption **A2** (Sect. 3.2), devices are not yet compromised when installed in a network.

Nevertheless, the spoofing of a targeted device fingerprint requires to generate new periodic communication and to disable existing periodic communication. The latter impacts the functionality of a device, which can consequently be detected as compromised by its user (e.g., missing periodic report) or its cloud service provider (e.g., missing reception of periodic heartbeat signal). In addition, spoofing a device type fingerprint has the only effect for the device to get assigned a different anomaly detection model than the one it was supposed to. First, this means that the device will anyway have a restricted communication behavior as defined by the anomaly detection model of the spoofed type (this model may of course be less restrictive). Second, communication related to legitimate functionality of the device will trigger anomalies, as it is likely not included in the anomaly detection profile of the spoofed type.

Spoofing MAC address. D²IoT anomaly detection is based on layer-2 traffic involving a particular device, identified by its MAC address. An adversary who has compromised a device can attempt to evade detection by spoofing its MAC address in the packets it sends out. This naturally decreases its utility since it cannot receive responses from operations like scanning for vulnerable devices or command & control traffic that are typical for compromised devices.

Mimicking legitimate communication. An adversary can attempt to mimic the legitimate communication patterns of a compromised device to remain undetected. However, D²IoT builds device-type-specific detection models that are very restrictive because IoT devices have limited functionality. Considering our packet characteristics (protocol, packet size, port, etc.), it is difficult to mimic legitimate communication while achieving a malicious purpose, e.g., scanning, flooding, etc. Moreover, adversaries would have to develop device-type-specific models for mimicking communication patterns. This makes it significantly harder to develop large scale IoT malware that affects a wide range of IoT devices, e.g., Mirai.

Forging anomaly detection features (adversarial machine learning). Having access to the anomaly detection model, one can attempt to forge packets specifically meant to avoid detection, i.e., *adversarial examples*. There exist techniques to forge adversarial examples to neural networks [8, 44]. However, these apply to images [32, 16] and audio inputs [9, 57, 63], where objective functions for the optimization problem are easy to define. Forging adversarial examples consists of finding minimal modifications ϵ for an input x of class C such that $x + \epsilon$ is classified as $C' \neq C$. In contrast to image or audio processing, our features (symbols) are not raw but processed from packets. First, it means that modifications ϵ are computed for our symbolic representation of packets and are difficult to implement as packets while preserving their adversarial utility. Second, it is difficult to define the objective distance to minimize in order to achieve “small modifications” since modifying the value of one single packet characteristic (protocol, port, etc.) can change the function of a packet entirely.

Poisoning federated learning. The learning of our anomaly detection models involves many Security Gateways providing training data. For initial model training, it is reasonable to assume we only use legitimate network traffic accord-

ing to assumption **A1** (Sect. 3.2). However, this crowd-sourced setting is subject to poisoning attacks [59] during re-training. Malicious clients can use compromised training data aimed at modifying the anomaly detection model such that it eventually accepts anomalies [4]. Techniques have been developed to prevent poisoning attacks in local [50] and distributed learning settings [54]. Since federated learning is a hybrid approach in which a computation is delegated to clients, we can combine both prevention techniques. If the client device supports a suitable trusted execution environment, like Intel SGX [12] or trusted platform module, enforcement of local prevention methods can be verified remotely using *remote attestation* techniques [13].

8. DISCUSSION

Generalizability of device fingerprinting. Features that compose our device fingerprint have been defined to model periodic flows and to differentiate IoT devices having different periodic flows. This feature definition and the use of a specific classifier, kNN, was motivated in Sect. 4. As in any machine learning application, the efficiency of a feature set and a classifier can only be demonstrated for a specific task and a specific dataset (no free lunch theorem [61]).

To ensure generalizability, we defined fingerprint features and selected a kNN classifier without prior knowledge about communications of specific IoT devices. Consequently our features are independent from any dataset and more specifically from the data we later processed in experiments. Data-independent features and the machine learning method choice ensure generalizability of the fingerprinting technique [36]. We assessed this technique on a large set of 33 IoT devices (IP cameras, sensors, coffee machine, etc.) that we expect to be representative of any smart home IoT device. Consequently we expect the 98.2% accuracy obtained during fingerprinting evaluation (cf. Sect. 6.2) to be generalizable to any other IoT devices, too.

Generalizability of anomaly detection. We focused our evaluation on the most well-known and nefarious IoT botnet so far: Mirai [1]. However, D²IoT is likely effective also in detecting other botnet malware like Persirai [62], Hajime [15], etc. Conceptually, D²IoT’s anomaly detection leverages deviations in the behavior of infected IoT devices caused by the malware. Such deviations will be observable for any botnet malware that performs actions like scanning for vulnerable devices or performing active attacks.

Scalability. Traditional anomaly detection approaches utilizing a single model for modeling benign behavior easily suffer from increasing false positive rates or decreasing sensitivity when the number of different types of behaviors (i.e., device types) captured by the model grows. This makes them unsuitable for real-world deployments with hundreds or thousands of different device types. Our solution, however, does not have this drawback, as it uses a dedicated detection model for each device type. Each of these models focuses solely on the characteristic behavior of one single device type, resulting in more specific and accurate behavioral models, independent of the number of different device types handled by the system. The detection accuracy of D²IoT will therefore remain high even if scaled to handle numerous different device types.

Evolution of IoT device behavior. The behavior of an IoT device type can evolve due to, e.g., firmware updates that bring new functionality. This modifies its behavior

and may trigger false alarms for legitimate communication. We prevent these false alarms by correlating anomaly reports from all Security Gateways at the IoT Security Service. Assuming firmware updates would be propagated to many client networks in a short time, if alarms are reported from a large number of security gateways for the same device type in a short time, we can cancel the alarm and trigger re-learning of the corresponding device identification and anomaly detection models to adapt to this new behavior. To ensure that sudden widespread outbreaks of an IoT malware infection campaign are not erroneously interpreted as firmware updates, the canceling of an alarm can be confirmed by a human expert at the IoT Security Service. This should represent a small burden, as the roll-out of firmware updates is a relatively seldom event and can thus be handled manually.

9. RELATED WORK

9.1 Anomaly Detection in IoT Network

Several solutions have been proposed for the detection and prevention of intrusions in IoT networks [3, 22, 49], sensor networks [48] and industrial control systems [21, 25]. SVELTE [49] is an intrusion detection system for protecting IoT networks from already known attacks. It adapts existing detection techniques to IoT-specific protocols, e.g., 6LoWPAN. In contrast, D \ddot{I} O T performs dynamic detection of unknown attacks and only models legitimate network traffic. Jia *et al.* [22] proposed a context-based system to automatically detect sensitive actions in IoT platforms. This system is designed for patching vulnerabilities in appified IoT platforms such as Samsung SmartThings. It does not adapt to multi-vendor IoT systems while D \ddot{I} O T is platform independent.

Detecting anomalies in network traffic has a long history [19, 30, 31, 33, 45, 52, 56]. Existing approaches rely on analysing single network packets [30, 31] or clustering large numbers of packets [45, 48] to detected intrusions or compromised services. Some works have proposed, as we do, to model communication as a language [25, 52]. For instance, authors of [52] derive finite state automatons from layer 3-4 communication protocol specifications. Monitored packets are processed by the automaton to detect deviations from protocol specification or abnormally high usage of specific transitions. Automatons can only model short sequences of packets while we use GRU to model longer sequences, which enables the detection of stealthy attacks. Also, modeling protocol specification is coarse and leaves room for circumventing detection. In contrast, we use finer grained features for modeling packets. These are difficult to forge while preserving the adversarial utility of malicious packets. Finally, previous work did not tackle the problem of gathering data for training anomaly detection models. This is a tedious and long task considering the large number of IoT devices. D \ddot{I} O T integrates a crowdsourced federated learning solution to address the training of anomaly detection models.

Lately, recurrent neural networks (RNN) have been used for several anomaly-detection purposes. Most applications leverage long short-term memory (LSTM) networks for detecting anomalies in time series [35], aircraft data [41] or system logs [14]. One close application is the use of deep belief networks for mining DNS log data and detect infections in enterprise networks [42]. In contrast to these works, D \ddot{I} O T uses a different flavor of RNN, namely GRU, for anomaly

detection. Also previous security applications [14, 42] were targeted at offline analysis of log data, while D \ddot{I} O T operates in real-time, detecting anomalies in live network traffic.

9.2 Device-Type Identification

Early work in wireless communication fingerprinting targeted the identification of hardware- and driver-specific characteristics [7, 17, 37]. IoT-oriented device identification techniques leverage sensor-specific features [5, 58, 53, 20] to uniquely identify a device. Our identification technique is positioned between the former and latter approaches, providing the right granularity to passively identify *device types*.

Some solutions address device-type identification with the same granularity as we do [2, 39, 46], while considering different definitions of “type”. GTID [46] identifies the make and model of a device by analyzing the inter-arrival time of packets sent for a targeted type of traffic (e.g. Skype, ICMP, etc.). GTID requires a lot of traffic over several hours to identify a device’s type. Maiti *et al.* [34] introduced a device-type identification technique relying on analysis of encrypted WiFi traffic. A Random Forest classifier is trained with features extracted from a long sequence of WiFi frames. The technique was evaluated on 10 IoT devices and required at least 30,000 frames to be effective. Under a standby state of operation, an IoT device can take days to generate such a volume of traffic. IoT Sentinel [40] leverages the burst of network traffic typical from the setup phase of an IoT device to identify its type. While accurate and requiring only two minutes of monitoring, IoT Sentinel only operates when a device is first installed to a network. Meidan *et al.* [39] analyze TCP sessions to identify generic types of IoT devices, i.e., *smoke sensor*, *baby monitor*, etc. The observation of at least 20 TCP sessions was required to reach acceptable accuracy on 17 devices. Authors reported that 1/3 of their IoT devices did not produce any TCP sessions without user interactions (standby mode), and for the remaining 2/3 the mean inter-arrival time of TCP sessions was up to 5 minutes, requiring over one hour and a half to be identified.

State-of-the-Art methods for device-type identification are supervised and require labeled data to be trained. D \ddot{I} O T is not restricted to a finite set of pre-learned device types. It creates abstract device types, learns their fingerprints and adapts autonomously when new types are discovered. D \ddot{I} O T is also not restricted to a specific type of dense network traffic. It is the first technique to identify IoT device types based on their background periodic communication. Consequently and in contrast to previous work, it identifies the type of an IoT device under *any state of operation*.

Finally some security solutions with a design close to D \ddot{I} O T have been proposed by the industry, e.g., IoT guardian from Zingbox [10]. However, IoT guardian does not propose any concrete implementation for an unsupervised device identification technique nor any novel solution to anomaly detection. Moreover, IoT guardian relies on partial deep packet inspection which prevents operation on encrypted communications. D \ddot{I} O T does not present such a limitation.

10. CONCLUSIONS

In this paper we introduced D \ddot{I} O T : a self-learning system for detecting compromised devices in IoT networks. Our solution relies on novel automated techniques for *device-type identification* and *device-type-specific anomaly detec-*

tion. D²IoT does not require any human intervention or labeled data to operate. It learns device-type identification models and anomaly detection models autonomously, using unlabeled crowdsourced data captured in client IoT networks. We evaluated the accuracy of D²IoT’s device-type identification method on a large dataset comprising 33 real-world IoT devices showing that it quickly learns (in a few hours) accurate (98%) identification models. We demonstrated the efficacy of anomaly detection in detecting a large set of malicious behavior from devices infected by the Mirai malware. D²IoT detected 94% of attacks in 2 seconds on average and without raising any false alarm when evaluated in a real-world deployment.

Acknowledgment

This work was supported in part by the Intel Collaborative Institute for Collaborative Autonomous and Resilient Systems (ICRI-CARS) and by the SELIoT project and the Academy of Finland under the Wi-FiUS program (grant 309994). We would like to thank Cisco Systems, Inc. for their support of this work. We thank Minh Hoang Dang from Le Quy Don Technical University for initial discussions and help in building our GRU models.

11. REFERENCES

- [1] M. Antonakakis, T. April, M. Bailey, M. Bernhard, E. Bursztein, J. Cochran, Z. Durumeric, J. A. Halderman, L. Invernizzi, M. Kallitsis, D. Kumar, C. Lever, Z. Ma, J. Mason, D. Menscher, C. Seaman, N. Sullivan, K. Thomas, and Y. Zhou. Understanding the mirai botnet. In *26th USENIX Security Symposium (USENIX Security 17)*, pages 1093–1110, Vancouver, BC, 2017. USENIX Association.
- [2] N. Apthorpe, D. Reisman, and N. Feamster. A smart home is no castle: Privacy vulnerabilities of encrypted iot traffic. *arXiv preprint arXiv:1705.06805*, 2017.
- [3] D. Barrera, I. Molloy, and H. Huang. IDIoT: Securing the Internet of Things like it’s 1994. *ArXiv e-prints*, Dec. 2017. <http://adsabs.harvard.edu/abs/2017arXiv171203623B>.
- [4] B. Biggio, B. Nelson, and P. Laskov. Poisoning attacks against support vector machines. In *Proceedings of the 29th International Conference on International Conference on Machine Learning*, pages 1467–1474. Omnipress, 2012.
- [5] H. Bojinov, Y. Michalevsky, G. Nakibly, and D. Boneh. Mobile device identification via sensor fingerprinting. *arXiv preprint:1408.1416*, 2014.
- [6] V. Brik, S. Banerjee, M. Gruteser, and S. Oh. Wireless device identification with radiometric signatures. In *International Conference on Mobile Computing and Networking*, pages 116–127. ACM, 2008.
- [7] J. Cache. Fingerprinting 802.11 implementations via statistical analysis of the duration field. *Uninformed*, 5, 2006.
- [8] N. Carlini and D. Wagner. Towards evaluating the robustness of neural networks. In *Security and Privacy (SP), 2017 IEEE Symposium on*, pages 39–57. IEEE, 2017.
- [9] N. Carlini and D. Wagner. Audio Adversarial Examples: Targeted Attacks on Speech-to-Text. *ArXiv e-prints*, Jan. 2018. <http://adsabs.harvard.edu/abs/2018arXiv180101944C>.
- [10] G. Cheng, P.-C. Yip, Z. Xiao, R. Xia, and M. Wang. Packet analysis based iot management, Oct. 13 2016. US Patent App. 15/087,861.
- [11] J. Chung, Ç. Gülçehre, K. Cho, and Y. Bengio. Empirical evaluation of gated recurrent neural networks on sequence modeling. *CoRR*, abs/1412.3555, 2014. <http://arxiv.org/abs/1412.3555>.
- [12] V. Costan and S. Devadas. Intel SGX explained. *IACR Cryptology ePrint Archive*, 2016:86, 2016.
- [13] G. Dessouky, S. Zeitouni, T. Nyman, A. Paverd, L. Davi, P. Koeberl, N. Asokan, and A.-R. Sadeghi. LO-FAT: Low-overhead control flow attestation in hardware. In *Design Automation Conference (DAC), 2017 54th ACM/EDAC/IEEE*, pages 1–6. IEEE, 2017.
- [14] M. Du, F. Li, G. Zheng, and V. Srikumar. Deeplog: Anomaly detection and diagnosis from system logs through deep learning. In *Proceedings of the 2017 ACM SIGSAC Conference on Computer and Communications Security, CCS ’17*, pages 1285–1298. ACM, 2017. <http://doi.acm.org/10.1145/3133956.3134015>.
- [15] S. Edwards and I. Profetis. Hajime: Analysis of a decentralized internet worm for IoT devices. Technical report, Rapidity Networks, 2016.
- [16] I. Evtimov, K. Eykholt, E. Fernandes, T. Kohno, B. Li, A. Prakash, A. Rahmati, and D. Song. Robust physical-world attacks on machine learning models. *arXiv preprint arXiv:1707.08945*, 2017.
- [17] J. Franklin, D. McCoy, P. Tabriz, V. Neaogoe, J. Van Randwyk, and D. Sicker. Passive data link layer 802.11 wireless device driver fingerprinting. In *USENIX Security Symposium*. USENIX, 2006.
- [18] J. Gamblin. Mirai source code, July 2017. <https://github.com/jgamblin/Mirai-Source-Code>.
- [19] P. Garcia-Teodoro, J. Diaz-Verdejo, G. Maciá-Fernández, and E. Vázquez. Anomaly-based network intrusion detection: Techniques, systems and challenges. *computers & security*, 28(1-2):18–28, 2009.
- [20] I. Haider, M. Höberl, and B. Rinner. Trusted sensors for participatory sensing and IoT applications based on physically unclonable functions. In *Proceedings of the 2Nd ACM International Workshop on IoT Privacy, Trust, and Security, IoTPTS ’16*, pages 14–21. ACM, 2016.
- [21] W. Jardine, S. Frey, B. Green, and A. Rashid. Senami: Selective non-invasive active monitoring for ics intrusion detection. In *Proceedings of the 2Nd ACM Workshop on Cyber-Physical Systems Security and Privacy, CPS-SPC ’16*, pages 23–34, 2016.
- [22] Y. J. Jia, Q. A. Chen, S. Wang, A. Rahmati, E. Fernandes, Z. M. Mao, and A. Prakash. ContextIoT: Towards providing contextual integrity to appified IoT platforms. In *24th Annual Network & Distributed System Security Symposium (NDSS)*, feb 2017.
- [23] Z. Jiang, A. Balu, C. Hegde, and S. Sarkar. Collaborative deep learning in fixed topology networks. In *Advances in Neural Information Processing Systems*, pages 5906–5916, 2017.
- [24] keras.io. Gated recurrent unit, 2018. <https://keras.io/layers/recurrent/>.

- [25] A. Kleinmann and A. Wool. Automatic construction of statechart-based anomaly detection models for multi-threaded scada via spectral analysis. In *Proceedings of the 2Nd ACM Workshop on Cyber-Physical Systems Security and Privacy*, CPS-SPC '16, pages 1–12. ACM, 2016.
- [26] T. Kohno, A. Broido, and K. C. Claffy. Remote physical device fingerprinting. *IEEE Trans. Dependable Secure Comput.*, 2(2):93–108, April 2005.
- [27] C. Koliass, G. Kambourakis, A. Stavrou, and J. Voas. DDoS in the IoT: Mirai and other botnets. *Computer*, 50(7):80–84, 2017.
- [28] J. Konečný, B. McMahan, F. X. Yu, P. Richtárik, A. T. Suresh, and D. Bacon. Federated learning: Strategies for improving communication efficiency. *CoRR*, abs/1610.05492, 2016.
- [29] B. Krebs. KrebsOnSecurity hit with record DDoS. <https://krebsonsecurity.com/2016/09/krebsonsecurity-hit-with-record-ddos/>.
- [30] C. Kruegel and G. Vigna. Anomaly detection of web-based attacks. In *Proceedings of the 10th ACM conference on Computer and communications security*, pages 251–261. ACM, 2003.
- [31] C. Krügel, T. Toth, and E. Kirda. Service specific anomaly detection for network intrusion detection. In *Proceedings of the 2002 ACM symposium on Applied computing*, pages 201–208. ACM, 2002.
- [32] A. Kurakin, I. Goodfellow, and S. Bengio. Adversarial examples in the physical world. *arXiv preprint arXiv:1607.02533*, 2016.
- [33] A. Lazarevic, L. Ertöz, V. Kumar, A. Ozgur, and J. Srivastava. A comparative study of anomaly detection schemes in network intrusion detection. In *Proceedings of the 2003 SIAM International Conference on Data Mining*, pages 25–36. SIAM, 2003.
- [34] R. R. Maiti, S. Siby, R. Sridharan, and N. O. Tippenhauer. Link-layer device type classification on encrypted wireless traffic with cots radios. In *European Symposium on Research in Computer Security*, pages 247–264. Springer, 2017.
- [35] P. Malhotra, L. Vig, G. Shroff, and P. Agarwal. Long short term memory networks for anomaly detection in time series. In *Proceedings*, page 89. Presses universitaires de Louvain, 2015.
- [36] S. Marchal, G. Armano, T. Gröndahl, K. Saari, N. Singh, and N. Asokan. Off-the-hook: An efficient and usable client-side phishing prevention application. *IEEE Transactions on Computers*, 66(10):1717–1733, 2017.
- [37] C. Maurice, S. Onno, C. Neumann, O. Heen, and A. Francillon. Improving 802.11 fingerprinting of similar devices by cooperative fingerprinting. In *Proceedings of the 2013 International Conference on Security and Cryptography (SECRYPT)*, pages 1–8, 2013.
- [38] B. McMahan, E. Moore, D. Ramage, S. Hampson, and B. A. y Arcas. Communication-efficient learning of deep networks from decentralized data. In *Proceedings of the 20th International Conference on Artificial Intelligence and Statistics*, pages 1273–1282, 2017.
- [39] Y. Meidan, M. Bohadana, A. Shabtai, M. Ochoa, N. O. Tippenhauer, J. D. Guarnizo, and Y. Elovici. Detection of unauthorized IoT devices using machine learning techniques. *CoRR*, abs/1709.04647, 2017.
- [40] M. Miettinen, S. Marchal, I. Hafeez, N. Asokan, A. Sadeghi, and S. Tarkoma. IoT Sentinel: Automated Device-Type Identification for Security Enforcement in IoT. In *Proc. 37th IEEE International Conference on Distributed Computing Systems (ICDCS 2017)*, June 2017.
- [41] A. Nanduri and L. Sherry. Anomaly detection in aircraft data using recurrent neural networks (rnn). In *Integrated Communications Navigation and Surveillance (ICNS), 2016*, pages 5C2–1. IEEE, 2016.
- [42] A. Oprea, Z. Li, T.-F. Yen, S. H. Chin, and S. Alrwais. Detection of early-stage enterprise infection by mining large-scale log data. In *Dependable Systems and Networks (DSN), 2015 45th Annual IEEE/IFIP International Conference on*, pages 45–56. IEEE, 2015.
- [43] Y. M. P. Pa, S. Suzuki, K. Yoshioka, T. Matsumoto, T. Kasama, and C. Rossow. IoTPOT: A novel honeypot for revealing current IoT threats. *Journal of Information Processing*, 24(3):522–533, 2016.
- [44] N. Papernot, P. McDaniel, I. Goodfellow, S. Jha, Z. B. Celik, and A. Swami. Practical black-box attacks against machine learning. In *Proceedings of the 2017 ACM on Asia Conference on Computer and Communications Security*, pages 506–519. ACM, 2017.
- [45] L. Portnoy, E. Eskin, and S. Stolfo. Intrusion detection with unlabeled data using clustering. In *In Proceedings of ACM CSS Workshop on Data Mining Applied to Security (DMSA-2001)*. Citeseer, 2001.
- [46] S. V. Radhakrishnan, A. S. Uluagac, and R. Beyah. GTID: A technique for physical device and device type fingerprinting. *IEEE Transactions on Dependable and Secure Computing*, 12(5):519–532, 2015.
- [47] Radware. BrickerBot results in PDoS attack. <https://security.radware.com/ddos-threats-attacks/brickerbot-pdos-permanent-denial-of-service/>.
- [48] S. Rajasegarar, C. Leckie, and M. Palaniswami. Hyperspherical cluster based distributed anomaly detection in wireless sensor networks. *Journal of Parallel and Distributed Computing*, 74(1):1833–1847, 2014.
- [49] S. Raza, L. Wallgren, and T. Voigt. Svelte: Real-time intrusion detection in the internet of things. *Ad hoc networks*, 11(8):2661–2674, 2013.
- [50] B. I. Rubinstein, B. Nelson, L. Huang, A. D. Joseph, S.-h. Lau, S. Rao, N. Taft, and J. Tygar. Antidote: understanding and defending against poisoning of anomaly detectors. In *Proceedings of the 9th ACM SIGCOMM conference on Internet measurement*, pages 1–14. ACM, 2009.
- [51] R. J. Samworth et al. Optimal weighted nearest neighbour classifiers. *The Annals of Statistics*, 40(5):2733–2763, 2012.
- [52] R. Sekar, A. Gupta, J. Frullo, T. Shanbhag, A. Tiwari, H. Yang, and S. Zhou. Specification-based anomaly detection: a new approach for detecting network intrusions. In *Proceedings of the 9th ACM conference on Computer and communications security*, pages 265–274. ACM, 2002.
- [53] Y. Sharaf-Dabbagh and W. Saad. On the authentication of devices in the Internet of Things. In

Proceedings of the 17th IEEE International Symposium on A World of Wireless, Mobile and Multimedia Networks (WoWMoM), pages 1–3. IEEE, 2016.

- [54] S. Shen, S. Tople, and P. Saxena. Auror: Defending against poisoning attacks in collaborative deep learning systems. In *Proceedings of the 32Nd Annual Conference on Computer Security Applications, ACSAC '16*, pages 508–519. ACM, 2016.
- [55] V. Smith, C.-K. Chiang, M. Sanjabi, and A. S. Talwalkar. Federated multi-task learning. In I. Guyon, U. V. Luxburg, S. Bengio, H. Wallach, R. Fergus, S. Vishwanathan, and R. Garnett, editors, *Advances in Neural Information Processing Systems*, pages 4427–4437. 2017.
- [56] R. Sommer and V. Paxson. Outside the closed world: On using machine learning for network intrusion detection. In *Security and Privacy (SP), 2010 IEEE Symposium on*, pages 305–316. IEEE, 2010.
- [57] T. Vaidya, Y. Zhang, M. Sherr, and C. Shields. Cocaine noodles: exploiting the gap between human and machine speech recognition. *WOOT*, 15:10–11, 2015.
- [58] T. Van Goethem, W. Scheepers, D. Preuveneers, and W. Joosen. Accelerometer-based device fingerprinting for multi-factor mobile authentication. In *Proceedings of the 8th International Symposium on Engineering Secure Software and Systems, ESSoS 2016*, pages 106–121. Springer International Publishing, 2016.
- [59] G. Wang, T. Wang, H. Zheng, and B. Y. Zhao. Man vs. machine: Practical adversarial detection of malicious crowdsourcing workers. In *USENIX Security Symposium*, pages 239–254, 2014.
- [60] S. Winograd. On computing the discrete fourier transform. *Mathematics of computation*, 32(141):175–199, 1978.
- [61] D. H. Wolpert and W. G. Macready. No free lunch theorems for optimization. *IEEE transactions on evolutionary computation*, 1(1):67–82, 1997.
- [62] T. Yeh, D. Chiu, and K. Lu. Persirai: New internet of things (IoT) botnet targets IP cameras. <https://blog.trendmicro.com/trendlabs-security-intelligence/persirai-new-internet-things-iot-botnet-targets-ip-cameras/>.
- [63] G. Zhang, C. Yan, X. Ji, T. Zhang, T. Zhang, and W. Xu. Dolphinattack: Inaudible voice commands. In *Proceedings of the 2017 ACM SIGSAC Conference on Computer and Communications Security*, pages 103–117. ACM, 2017.

APPENDIX

A. EXAMPLE PERIODIC FLOW INFERENCE

To illustrate the periodicity of IoT device communication, Figure 7 shows the plot of binary time series extracted from flows of a D-LinkCamDCS935LA IP camera. We see that all depicted flows are periodic. The computation of DFT and autocorrelation on these time series provides the following results:

ARP: (period:55, r:0.735, rn:0.857)
 port 443: (period:55, r:0.857, rn:1.102)
 port 5353: (period:25, r:2.171, rn:4.399)
 port 62976: (period:30, r:0.969, rn:0.969)

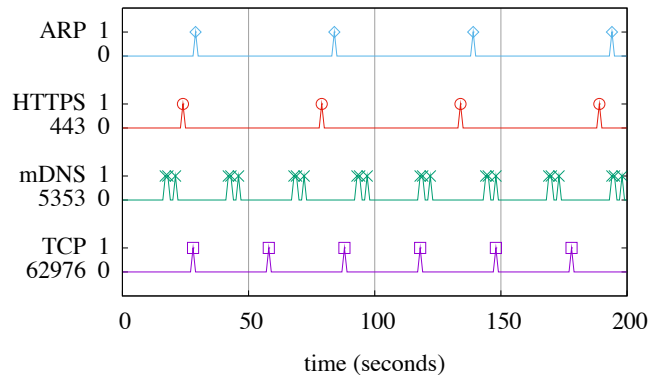


Figure 7: Four binary time series extracted from periodic flows of a D-LinkCamDCS935LA IP camera. The flows correspond to ARP protocol, HTTPS (port 443), mDNS (port 5353) and TCP port 62976. All are periodic.

We see that our method is able to accurately infer all periods observed in Figure 7. The flow on TCP port 62976 has the most stable period (30s.) as highlighted by the values $r = rn \approx 1$. ARP and HTTPS (port 443) have both a less stable period of 55s., as highlighted by lower r values and a larger difference between r and rn . We also inferred the 25s. period of the mDNS flow (port 5353). But as we can observe in Figure 7, there are three different signals having a 25s. periodicity on this flow. This aspect is captured in period inference by rendering high r and rn values, i.e. far larger than 1. These results show that the introduced periodic flow inference method detects periodic flows, accurately infer their period and characterize them with r and rn metrics.

B. DEVICE-TYPE IDENTIFICATION FEATURES

Table 5 presents the 33 features that compose fingerprints used for device-type identification.

C. IOT DEVICE ASSIGNMENT TO TYPES

Table 6 presents the device types created during device type identification and the affectation of each IoT device to these types.

D. IOT DEVICE LIST

Table 7 presents the 33 IoT devices used during evaluation of DIoT.

E. CONFUSION MATRIX DEVICE-TYPE IDENTIFICATION

Table 8 is the confusion matrix obtained from device-type identification evaluation.

F. EXAMINED MIRAI ATTACK VECTORS

Table 9 shows the different attack scenarios used in collecting the *attack* dataset.

Table 5: 33 features (4 categories) used for device-type identification. # represents a count.

Category	f	Description
periodic flows	1	# periodic flows
	2	# periodic flows (protocol \leq layer 4)
	3	Mean periods per flow
	4	SD periods per flow
	5	# flows having only one period
	6	# flows having multiple periods
	7	# periodic flows with static source port
	8	Mean frequency source port change
	9	SD frequency source port change
period accuracy	10	# periods inferred in all sub-captures
	11	Mean period inference success
	12	SD period inference success
period duration	13	# periods $\in [5s.; 29s.]$
	14	# periods $\in [30s.; 59s.]$
	15	# periods $\in [60s.; 119s.]$
	16	# periods $\in [120s.; 600s.]$
period stability	17	# Mean(r) $\in [0.2; 0.7[$
	18	# Mean(r) $\in [0.7; 1[$
	19	# Mean(r) $\in [1; 2[$
	20	# Mean(r) $\in [2; +\infty[$
	21	# SD(r) $\in [0; 0.02[$
	22	# SD(r) $\in [0.02; 0.1[$
	23	# SD(r) $\in [0.1; +\infty[$
	24	# Mean(rn) $\in [0.2; 0.7[$
	25	# Mean(rn) $\in [0.7; 1[$
	26	# Mean(rn) $\in [1; 2[$
	27	# Mean(rn) $\in [2; +\infty[$
	28	# SD(rn) $\in [0; 0.02[$
	29	# SD(rn) $\in [0.02; 0.1[$
	30	# SD(rn) $\in [0.1; +\infty[$
	31	# Mean(rn) - Mean(r) $\in [0; 0.02[$
	32	# Mean(rn) - Mean(r) $\in [0.02; 0.1[$
	33	# Mean(rn) - Mean(r) $\in [0.1; +\infty[$

Table 6: Affection of 33 IoT devices to 23 DIoT device types during evaluation (Sect. 6.2)

device-type	IoT device
<i>type#01</i>	ApexisCam
<i>type#02</i>	CamHi
<i>type#03</i>	D-LinkCamDCH935L
<i>type#04</i>	D-LinkCamDCS930L
	D-LinkCamDCS932L
<i>type#05</i>	D-LinkDoorSensor
	D-LinkSensor
	D-LinkSiren
	D-LinkSwitch
	D-LinkWaterSensor
<i>type#06</i>	EdimaxCamIC3115
	EdimaxCamIC3115(2)
<i>type#07</i>	EdimaxPlug1101W
	EdimaxPlug2101W
<i>type#08</i>	EdnetCam
<i>type#09</i>	EdnetGateway
<i>type#10</i>	HomeMaticPlug
<i>type#11</i>	Lightify
<i>type#12</i>	SmcRouter
<i>type#13</i>	TPLinkPlugHS100
	TPLinkPlugHS110
<i>type#14</i>	UbntAirRouter
<i>type#15</i>	WansviewCam
<i>type#16</i>	WemoLink
<i>type#17</i>	WemoInsightSwitch
	WemoSwitch
<i>type#18</i>	HueSwitch
<i>type#19</i>	AmazonEcho
<i>type#20</i>	AmazonEchoDot
<i>type#21</i>	GoogleHome
<i>type#22</i>	Netatmo
<i>type#23</i>	iKettle2
	SmarterCoffee

Table 7: IoT devices used in the *background*, *activity*, *deployment* and *attack* datasets and their connectivity technologies

Identifier	Device Model	WiFi	Ethernet	Other	Background	Activity	Deployment	Attack
AmazonEcho	Amazon Echo	●	○	○	○	●	●	○
AmazonEchoDot	Amazon Echo Dot	●	○	○	○	●	○	○
ApexisCam	Apexis IP Camera APM-J011	●	●	○	●	●	○	○
CamHi	Cooau Megapixel IP Camera	●	●	○	●	●	○	○
D-LinkCamDCH935L	D-Link HD IP Camera DCH-935L	●	○	○	●	●	○	○
D-LinkCamDCS930L	D-Link WiFi Day Camera DCS-930L	●	●	○	●	○	●	●
D-LinkCamDCS932L	D-Link WiFi Camera DCS-932L	●	●	○	●	○	●	●
D-LinkDoorSensor	D-Link Door & Window sensor	○	○	●	●	●	○	○
D-LinkSensor	D-Link WiFi Motion sensor DCH-S150	●	○	○	●	●	●	○
D-LinkSiren	D-Link Siren DCH-S220	●	○	○	●	●	○	○
D-LinkSwitch	D-Link Smart plug DSP-W215	●	○	○	●	●	●	○
D-LinkWaterSensor	D-Link Water sensor DCH-S160	●	○	○	●	●	○	○
EdimaxCamIC3115	Edimax IC-3115W Smart HD WiFi Network Camera	●	●	○	●	●	○	○
EdimaxCamIC3115(2)	Edimax IC-3115W Smart HD WiFi Network Camera	●	●	○	●	●	○	○
EdimaxPlug1101W	Edimax SP-1101W Smart Plug Switch	●	○	○	●	●	●	●
EdimaxPlug2101W	Edimax SP-2101W Smart Plug Switch	●	○	○	●	●	●	●
EdnetCam	Ednet Wireless indoor IP camera Cube	●	●	○	●	●	○	○
EdnetGateway	Ednet.living Starter kit power Gateway	●	○	●	●	●	●	○
GoogleHome	Google Home	●	○	○	●	○	●	○
HomeMaticPlug	Homematic pluggable switch HMIP-PS	○	○	●	●	●	○	○
HueSwitch	Philips Hue Light Switch PTM 215Z	○	○	●	●	●	●	○
iKettle2	Smarter iKettle 2.0 water kettle SMK20-EU	●	○	○	●	●	●	○
Lightify	Osram Lightify Gateway	●	○	●	●	●	●	○
Netatmo	Netatmo weather station with wind gauge	●	○	●	●	○	●	○
SmarterCoffee	Smarter SmarterCoffee coffee machine SMC10-EU	●	○	○	●	●	●	○
SmcRouter	SMC router SMCWBR14S-N4 EU	●	●	○	●	●	○	○
TP-LinkPlugHS100	TP-Link WiFi Smart plug HS100	●	○	○	●	●	○	○
TP-LinkPlugHS110	TP-Link WiFi Smart plug HS110	●	○	○	●	●	○	○
UbntAirRouter	Ubnt airRouter HP	●	●	○	●	●	○	●
WansviewCam	Wansview 720p HD Wireless IP Camera K2	●	○	○	●	●	○	○
WeMoInsightSwitch	WeMo Insight Switch model F7C029de	●	○	○	●	●	○	○
WeMoLink	WeMo Link Lighting Bridge model F7C031vf	●	○	●	●	●	○	○
WeMoSwitch	WeMo Switch model F7C027de	●	○	○	●	●	○	○

Table 8: Confusion matrix for device-type identification. Obtained with 10 repetitions of 4-fold cross validation. Columns represent predicted labels and rows actual labels.

	#01	#02	#03	#04	#05	#06	#07	#08	#09	#10	#11	#12	#13	#14	#15	#16	#17	#18	#19	#20	#21	#22	#23
type#01	480	0	0	0	0	0	0	0	0	30	0	0	0	0	0	0	0	0	0	0	0	0	0
type#02	24	1240	0	10	3	5	0	0	16	103	0	0	0	3	50	0	26	0	0	0	0	0	0
type#03	0	0	3736	0	0	10	0	0	0	0	0	24	0	0	0	0	0	0	0	0	0	0	0
type#04	0	0	0	2775	4	39	0	0	1	42	0	14	5	0	0	0	0	0	0	0	0	0	0
type#05	0	0	0	2	8707	12	0	0	10	19	0	0	0	0	0	0	0	0	0	0	0	0	0
type#06	0	0	0	10	0	3756	0	0	6	0	0	0	0	0	0	0	0	0	0	8	0	0	0
type#07	0	10	0	0	0	2	394	0	1	0	1	2	0	0	0	0	0	0	0	0	0	0	0
type#08	0	0	0	0	0	10	0	7390	0	0	0	0	0	0	0	0	0	0	0	0	0	0	0
type#09	0	0	0	0	0	0	0	0	2619	21	0	0	0	0	0	0	0	0	0	0	0	0	0
type#10	0	0	0	0	0	0	0	0	2	7323	0	0	0	17	0	0	0	0	0	0	0	0	8
type#11	0	0	0	13	38	30	0	0	0	1	2581	4	0	0	0	3	0	0	0	0	0	0	0
type#12	0	0	0	10	0	35	0	0	0	0	0	1955	0	0	0	0	0	0	0	0	0	0	0
type#13	0	0	0	0	0	0	0	0	0	21	0	0	3470	14	0	0	5	0	0	0	0	0	20
type#14	0	3	0	9	0	0	0	0	0	39	0	0	11	350	0	0	0	0	0	10	0	0	28
type#15	0	4	0	20	2	0	0	0	0	17	0	0	10	1412	0	0	0	0	0	0	0	0	5
type#16	0	0	0	2	0	3	0	0	0	0	0	18	0	0	0	2437	0	0	0	0	0	0	0
type#17	0	20	0	0	0	0	0	0	0	6	0	0	10	0	0	0	3884	0	0	0	0	0	0
type#18	0	0	0	50	0	0	0	0	12	0	1	0	0	0	0	12	1715	0	0	0	0	0	0
type#19	0	0	0	0	0	0	0	10	0	0	0	0	0	0	0	0	0	870	0	0	0	0	0
type#20	0	0	0	0	0	0	0	0	0	0	0	0	0	0	0	0	0	0	870	0	0	0	0
type#21	0	0	0	0	0	0	0	0	0	1	0	0	0	2	0	0	0	0	0	0	1710	0	17
type#22	0	0	0	0	0	0	0	0	0	0	0	0	0	0	0	6	0	0	0	2	0	292	0
type#23	0	0	0	0	0	0	0	0	0	0	0	0	0	1	0	0	0	0	0	0	10	0	1189

Table 9: Attack scenarios in the *attack* dataset.

Scenario	Description
scanning	Only scanning enabled
udp	UDP flood
syn	SYN flood
ack	ACK flood
udpplain	UDP flood with less options
vse	Valve source engine specific flood
dns	DNS resolver flood
greip	GRE IP flood
greeth	GRE Ethernet flood
http	HTTP flood

Source: https://www.nanog.org/sites/default/files/1_Winward_Mirai_The_Rise.pdf